IJC Heart & Vasculature 28 (2020) 100534

Contents lists available at ScienceDirect

IJC Heart & Vasculature

journal homepage: www.journals.elsevier.com/ijc-heart-and-vasculature

Pharmacological inhibition of sodium-proton-exchanger subtype 3-mediated sodium absorption in the gut reduces atrial fibrillation susceptibility in obese spontaneously hypertensive rats

Benedikt Linz [a,b,1,*], Mathias Hohl [a,1], Ricardo Mishima [c], Arnela Saljic [b], Dennis H. Lau [c], Thomas Jespersen [b], Ulrich Schotten [d], Prashanthan Sanders [c], Dominik Linz [a,c,d]

[a] Klinik für Innere Medizin III, Universität des Saarlandes, 66421 Homburg/Saar, Germany
[b] Department of Biomedical Sciences, Faculty of Health and Medical Sciences, University of Copenhagen, Copenhagen, Denmark.
[c] Centre for Heart Rhythm Disorders, South Australian Health and Medical Research Institute, Royal Adelaide Hospital, University of Adelaide, Adelaide, Australia
[d] University Maastricht, Cardiovascular Research Institute Maastricht (CARIM), the Netherlands

ARTICLE INFO

Article history:
Received 23 March 2020
Received in revised form 19 April 2020
Accepted 5 May 2020

Keywords:
Atrial fibrillation
Salt
Sodium-proton-exchanger Subtype 3 (NHE 3)
Intestinal sodium absorption

ABSTRACT

Background: Increased sodium uptake has been shown to contribute to hypertension and cardiac end-organ damage. The sodium-proton-exchanger subtype 3 (NHE3) is an important mediator of intestinal sodium absorption. Whether a reduction in intestinal sodium absorption can prevent the development of an atrial arrhythmogenic substrate in hypertension is unknown.

Methods: Eight-week-old obese spontaneously hypertensive rats (SHR-ob) were treated for six weeks with the gut-specific NHE3-inhibitor SAR (1-(β-D-glucopyranosyl)-3-{3-[(4S)-6,8-dichloro-2-methyl-1,2,3,4-tetrahydroiso-chinolin-4-yl]phenyl}urea, 1 mg/kg/d in chow, SHR-ob SAR, n = 7) and compared to aged-matched placebo-treated SHR-ob (SHR-ob PLAC, n = 8). Cardiac magnetic resonance imaging was performed at the end of the treatment period to assess atrial emptying function. Afterwards, local conduction disturbances and inducible atrial fibrillation (AF) duration were determined and histological analysis to quantify atrial fibrosis amount were performed.

Results: Inhibition of intestinal NHE3 by SAR increased fecal sodium excretion, resulted in marked changes in feces electrolyte concentrations and water content, reduced blood pressure and preserved atrial emptying function (active total percent emptying: SHR-ob SAR: 0.47 ± 0.05% vs. SHR-ob PLAC: 0.38 ± 0.007, $p < 0.0001$). Atrial fibrosis content was lower (21.4 ± 2.5% vs. 36.7 ± 1.2%, $p < 0.0001$) and areas of slow conduction were smaller (2.5 ± 0.09% vs. 5.3 ± 0.2%, $p < 0.0001$) in SHR-ob SAR compared to SHR-ob PLAC. Left atrial burst stimulation resulted in shorter inducible AF-durations in SHR-ob SAR compared to SHR-ob PLAC.

Conclusions: Reduction of intestinal sodium absorption and subsequent changes in feces milieu by pharmacological NHE3 inhibition in the gut preserved atrial emptying function and reduced AF susceptibility. Whether pharmacological NHE3 inhibition in the gut prevents AF in humans warrants further study.

1. Introduction

A Western lifestyle with high salt consumption can lead to hypertension [1,2] and may contribute to cardiac end-organ damage involving diastolic dysfunction and atrial fibrillation (AF). The World Health Organization technical report recommends a maximum daily intake of 5–6 g of salt for the general population [3]. Accordingly, salt restriction is also recommended in hypertension and heart failure guidelines of the European Society of Cardiology [4,5] but is not mentioned in the current AF guidelines [6].

It is notoriously difficult to sufficiently reduce salt in the human diet. When determining the relative contributions of dietary salt sources, salt added during food processing contributes 77% of total intake, 11.6% was derived from salt inherent to food, and water was a trivial source [7]. Theoretically, pharmacological modification of intestinal sodium absorption may represent an interesting way of pharmacological reduction of salt intake. Dietary salt is absorbed in the gastrointestinal tract. Intestinal salt and water

* Corresponding author at: University of Copenhagen, Faculty of Health and Medical Sciences, Department of Biomedical Sciences, Cardiac Physiology Laboratory, Panum Institutet, Blegdamsvej 3b, 2200 København, Denmark.
E-mail address: bene.linz@sund.ku.dk (B. Linz).
[1] Shared first authorship.

https://doi.org/10.1016/j.ijcha.2020.100534
2352-9067/

absorption in the gut is mainly regulated by the sodium proton exchanger subtype 3 (NHE3 also known as Slc9a3), which is highly expressed at the apical membrane of the intestine and colon [8,9]. Intestinal NHE3 may represent an interesting target for pharmacological intervention and may help to accomplish a truly low-salt intake from the gut. Pharmacological inhibition of the intestinal NHE3 has been shown to reduce intestinal sodium and water absorption and to result in reduction of blood pressure in hypertensive rat models [9,10] and attenuated progression of hypertensive renal and ventricular end-organ damage [11]. Theoretically, pharmacological NHE3 inhibition in the gut, initiated at a time when hypertension, metabolic syndrome and nephropathy are already fully established, may also prevent the progression of atrial arrhythmic substrates, which has not been investigated yet.

This study sought to delineate the effects of pharmacological inhibition of intestinal sodium absorption on development of an arrhythmogenic substrate for AF in obese spontaneously hypertensive rats (SHR-ob), which carry an additional mutation in the leptin receptor and express multiple abnormal phenotypes including hypertension, hyperinsulinemia and metabolic syndrome [9,11–15]. These rats show a blood pressure approximately corresponding to human hypertension and develop a progressive arrhythmogenic substrate for AF [12]. Whether NHE3 inhibition prevents the development of an atrial arrhythmic substrate is unclear.

2. Materials and methods

Animal experiments were conducted in accordance with the National Instructions of Health (NIH) Guide for the Care and Use of Laboratory Animals and with the Welfare guidelines and the German law for the protection of animals. The experimental protocol was reviewed and approved by the responsible institutional review committee, Darmstadt, Germany.

SAR (Sanofi Aventis Research: 1-(β-D-glucopyranosyl)-3-{3-[(4 S)-6,8-dichloro-2-methyl-1,2,3,4-tetrahydroiso-chinolin-4-yl]ph enyl}urea; molecular weight of 512.4 (free base)) is a novel NHE3 inhibitor with very low permeability and an oral bioavailability of <1%. An oral dose of 1 mg/kg corresponds with a plasma concentration of about 1 nmol/L. A dose-dependent inhibition study demonstrated a highly potent IC_{50} value of 22 nmol/L on rat NHE3 [9].

2.1. Animals

Male obese spontaneously hypertensive rats (SHR-ob, n = 15) were purchased from Charles River Germany GmbH (Sulzfeld, Germany). The animals were housed individually in standard cages and received standard chow diet (standard diet #1320, Altromin, Lage, Germany) and tap water ad libitum. At the age of eight weeks, rats were randomized into two groups. One group was treated for six weeks with the NHE3-inhibitor SAR (1 mg/kg/d in standard chow #1320, Altromin, Lage, Germany) (SHR-ob SAR, n = 7), the second group served as an untreated control fed with standard chow only (SHR-ob PLAC, n = 8).

For the determination of urinary and feces sodium-excretion, the rats were placed over 24 h in metabolic cages (Tecniplast S.p. a., Buguggiate, Italy) and the urine and feces were sampled. Ion concentrations in feces were measured (Hitachi 912 analyzer) and via flame photometry [8]. Water content in the feces was measured by the Karl Fischer method [8].

2.2. Magnetic resonance imaging

At the age of 14 weeks, rats were anesthetized with 1.5–2.5% isoflurane and cardiac LA-function was assessed by cardiac magnetic resonance imaging (MRI). All scans were acquired with a 7-T magnetic resonance imaging scanner (Bio Spec 70/30; Bruker Biospin GmbH, Ettlingen, Germany). Multi-slice short-axis cine imaging was performed from the upper left atrial roof to the apex with a slice thickness of 1.2 mm and an inter-slice gap of 0 mm. Orthogonal long axis cine imaging of the LA was acquired. LA boundaries were obtained in each short-axis image. The LA-volumes were then determined by Simpson's rule. LA-area was manually encircled. The point of insertion of the mitral valve leaflets was taken as the atrioventricular border. Pulmonary veins were excluded at their ostia and the left atrial appendage was excluded at its base. All dimensions were measured throughout the cardiac cycle. The cardiac cycle was divided into 10 equal phases with an interphase time difference of the spontaneous cycle length / 10. The MRI-images of all LAs were analyzed by the same investigator blinded to animal groupings. Representative MRI images of the left atrium and a further description of the methods is summarized in [12].

Minimal LA- (LAmin) and maximal LA-volume (LAmax) and their difference (cyclical change volume) were determined from the LA-volume/time curves. The minimal volume at the end of rapid passive emptying (LAre) and the volume before active emptying (LApc) were determined from the volume-time curves as described elsewhere [16,17]. LA-emptying function parameters (total percent emptying (LAmax-LAmin)/LAmax)), active percent emptying ((LApc-LAmin)/LApc), passive percent emptying (LAmax-LAre)/LAmax)) were computed [12]. LA-volume/body weight ratio (LA-volume index) was determined to normalize LA dimensions.

2.3. Electrophysiological studies

At the age of 14 weeks, all animals were anaesthetized with thiopental (Narcoren, 100 mg/kg i.p., Merial, Hallbergmoos, Germany), intubated and lungs were artificially ventilated. Surface ECG (lead II) was recorded via subcutaneous needle electrodes. A custom-made mapping electrode with 4*5 unipolar electrodes (1.0 mm inter-electrode distance) was placed on the LA free wall to analyze atrial conduction. Unipolar signals were recorded using a custom-made channel mapping amplifier (filtering bandwidth 0.1–408 Hz, sampling rate 1.0 kHz, A/D resolution 16bits). Unipolar pacing was performed from the surface of the left atrium (pulse width of 1 ms at twice the diastolic threshold, cycle length: 150 ms). Maps from 5 consecutive beats were analyzed. Local activation times were identified by maximum negative dV/dt in each unipolar electrogram. Local activation time differences were calculated between neighboring electrodes (conduction times). Conduction times of $\geq$ 3 ms (equivalent to conduction velocities $\leq$ 33 cm/s) were considered as being prolonged. Total-atrial activation time was defined as the time difference between the right atrial activation time, visualized by a custom made multiple action potential (MAP)-catheter (Franz-like electrode) next to the pacing electrode, and the latest left atrial activation time recorded by the mapping electrode during right atrial-pacing (cycle length: 150 ms). Atrial effective refractory period (AERP) was measured at a basic cycle length of 150 ms at the free wall of the LA. The mean of 3 AERP measurements was used for analysis. Susceptibility to AF was tested using repetitive 1 s bursts of stimuli (cycle length: 10 ms). When atrial electrograms showed a rapid atrial rate, cycle length < 70 ms and duration > 5 beats, AF was diagnosed. The duration of the longest of three induced subsequent episodes of AF was taken as inducible AF duration. After completion of electrophysiological measurements, the animals were sacrificed by quick excision of the hearts under continued deep anesthesia. The hearts were quickly excised, the atria carefully removed and transferred to 4% formaldehyde for subsequent histology.

2.4. Atrial histology

LA was fixed in buffered 4% formaldehyde for 24 h and embedded in paraffin for histological evaluation. Tissue sections of 5 μm were fixed at 56 °C overnight, deparaffinized, rehydrated and stained with hematoxylin and eosin (H&E) to determine cardiomyocyte diameter as a measure of cardiomyocyte hypertrophy and myocyte-myocyte distances within bundles as a measure of enhanced extracellular LA matrix formation and endomysial fibrosis formation. Representative images of the H&E staining of the left atrium and a further description of the methods is summarized in [12]. To visualize total tissue fibrosis amount, the sections were stained with Picro-Sirius Red. The percentage of the LA consisting of interstitial collagen was calculated as the ratio of Picro-Sirius-Red positively stained area over total LA tissue area, excluding blood vessels and the epi- and endocardial plane, using ImageJ 1.37a (National Institute of Health, USA). Fibrosis was quantified on three sections per atrium (6–8 fields per section).

2.5. Gene expression analyses

Gene expression analysis was performed in left atrial tissue by real-time polymerase chain reaction. Total RNA was extracted from whole left atrium by homogenizing in RLT buffer and by using RNeasy Mini columns (Qiagen). Genomic DNA impurities were removed by DNase treatment (DNA Removal Kit, Ambion), and cDNA was synthesized by reverse transcription (Life Science Technologies). Quantitative real-time polymerase chain reaction was performed using Taqman primers on an ABI Prism 7500 Sequence Detector (Applied Biosystems) and c(t) values obtained by using a respective software (SDS version 1.9). C(t) values were normalized to corresponding GAPDH controls. The deltaCt was used for statistical analysis and 2 deltaCt standardized to the control group was used for data presentation. Probes used to amplify the transcripts were as follows (purchased by Applied Biosystems): GAPDH (Rn99999916_s1), Transforming growth factor beta 1 (TGF-b1, Rn00572010_m1), collagen 1a1 (Col1a1, Rn01463848_m1), connective tissue growth factor (CTGF, Rn01537279_g1).

2.6. Statistics

Data are presented as means ± SEM and differences were tested for significance using an unpaired Student's *t*-test. A p-value of<0.05 was considered statistically significant.

3. Results

3.1. Feces milieu and blood pressure

Body weight was not changed by SAR (665 ± 11 g vs. 638 ± 15 g, n.s.). Water consumption was increased in NHE3 inhibitor–treated SHR-ob when compared with the placebo-treated SHR-ob (SHR-ob SAR: 68 ± 4 mL/kg per day vs. SHR-ob PLAC: 53 ± 3 mL/kg per day, $p < 0.05$). While sodium intake did not change (SHR-ob SAR: 0.64 ± 0.03 g/kg/d vs. SHR-ob PLAC: 0.65 ± 0.03 g/kg/d, n.s.), intestinal NHE3 inhibition by SAR resulted in increased feces electrolyte concentrations (Sodium: SHR-ob SAR: 54.3 ± 3.4 vs. SHR-ob PLAC: 17.5 ± 1.3 mmol/L, $p < 0.01$; Potassium: SHR-ob SAR: 29.9 ± 3.7 vs SHR-ob PLAC: 18.5 ± 1.1 mmol/L, $p = 0.06$; Calcium: SHR-ob SAR: 18.1 ± 0.9 vs. SHR-ob PLAC: 15.8 ± 2.5 mmol/L, n.s.; Chloride: SHR-ob SAR: 34 ± 2.6 vs. SHR-ob PLAC: 18.0 ± 0.7 mmol/L, $p < 0.01$). Higher feces sodium excretion (SHR-ob SAR: 0.19 ± 0.01 g/kg/d vs. SHR-ob PLAC: 0.05 ± 0.01 g/kg/d, $p < 0.01$) was associated with an increase in feces water content (SHR-ob SAR: 60.5 ± 0.9% vs. SHR-ob PLAC: 35.0 ± 1.3%, $p < 0.01$) in SAR treated SHR-ob animals.

The effects of intestinal NHE3 inhibition on blood pressure and left ventricular function in SHR-ob animals used in this study have been measured and published previously [9,11]. SAR significantly reduced intestinal sodium absorption and increased feces water content in SHR-ob, which was associated with a reduction of blood pressure from 222 ± 7 mmHg to 198 ± 2 mmHg ($p = 0.0001$) and a reduction in left ventricular end-diastolic pressure, while left ventricular end-systolic volume or left ventricular end-diastolic volume and ejection fraction were unchanged [9,11].

3.2. Left atrial structural remodeling

Total LA tissue fibrosis was increased in SHR-ob PLAC (36.7 ± 1.2%) compared to SHR-ob SAR (21.4 ± 2.5%, $p < 0.0001$; Fig. 1**A** and **B**). Myocyte-myocyte distances within bundles as a measure of enhanced extracellular LA matrix and endomysial fibrosis formation was enlarged in SHR-ob PLAC (3.20 ± 0.04 μm) compared to SHR-ob SAR (2.71 ± 0.06, $p < 0.0001$; Fig. 1**C**), while LA myocyte diameters as a measure of cardiomyocyte hypertrophy, was unchanged between both groups (SHR-ob PLAC: 18.3 ± 0.6 vs. SHR-ob SAR: 17.4 ± 0.5 μm, n.s. Fig. 1**D**). Gene expression of transforming growth factor beta 1 (TGFβ1), collagen 1a1 and connective tissue growth factor (CTGF) were lower in SHR-ob SAR than in SHR-ob PLAC (Table 1).

3.3. Effect of intestinal NHE3 inhibition on left atrial emptying function

In SHR-ob rats, SAR treatment demonstrated a better global LA-emptying function, as assessed by improved maximal LA volume index (SHR-ob SAR: 1.06 ± 0.001 μl/g*kg bodyweight vs. SHR-ob PLAC: 1.03 ± 0.003 μl/g*kg bodyweight, n.s.; Fig. 2**A**), total percent emptying (SHR-ob SAR: 0.47 ± 0.05% vs. SHR-ob PLAC: 0.38 ± 0.007, $p < 0.0001$; Fig. 2**B**) compared to placebo-treated SHR-ob. This preservation of better LA emptying function in SHR-ob SAR was mainly due to higher active percent emptying (SHR-ob SAR: 0.33 ± 0.01% vs. SHR-ob PLAC: 0.27 ± 0.01, $p = 0.0022$; Fig. 2**C**), while passive percent emptying was not changed (SHR-ob SAR: 0.21 ± 0.01% vs. SHR-ob PLAC: 0.21 ± 0.01, n.s.; Fig. 2**D**). Representative MRI images of 10 equal phases throughout the cardiac cycle at the level of the aortic valve are presented in Fig. 2**E**.

3.4. Left atrial electrophysiology

Atrial effective refractory period did not differ between SHR-ob PLAC and SHR-ob SAR (49.4 ± 0.6 ms vs. 50.1 ± 1.1, n.s.). Short episodes of AF could be induced by atrial burst stimulation in all SHR-ob PLAC rats (eight of eight) and all SHR-ob SAR rats (seven of seven). SAR treatment reduced total atrial activation time (SHR-ob PLAC: 17.13 ± 0.03 vs. SHR-ob SAR: 16.68 ± 0.04 ms, $p < 0.0001$; Fig. 3**A**) and the percentage of regions with slow conduction during rapid pacing (SHR-ob PLAC: 5.3 ± 0.24 vs. SHR-ob SAR: 2.5 ± 0.09%, $p < 0.0001$; Fig. 3**B**) in SHR-ob. The median duration of inducible AF was shorter in SAR-treated SHR-ob (8.85 ± 1.86 s) than in SHR-ob PLAC (30.0 ± 6.8 s, $p < 0.05$; Fig. 3**C**).

4. Discussion

Inhibition of NHE3-mediated intestinal sodium absorption resulted in changes in feces electrolyte concentration and increased water content, as well as reduced blood pressure in SHR-ob rats. This was associated with reduced interstitial fibrosis formation and reduced gene expression of TGFβ1, CTGF and collagen 1a1 in the atrium. As a result of these hemodynamic and atrial

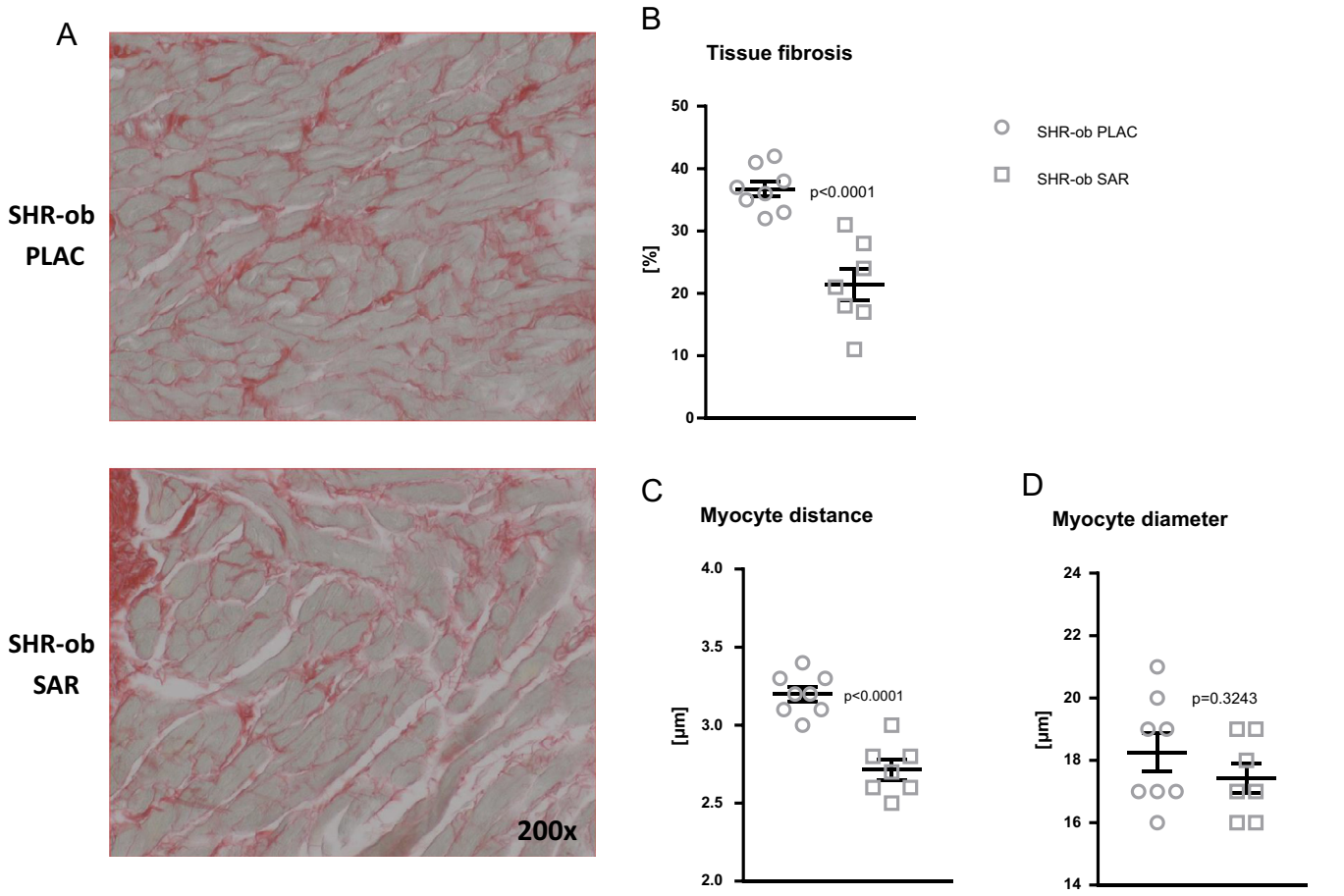

Fig. 1. Structural remodeling of the left atrium. A) Representative picture of Picro-Sirius red stained left atria. B) Quantification of total atrial tissue fibrosis by Picro-Sirius red staining. C) Myocyte-myocyte distances within bundles as a measure of enhanced extracellular LA matrix formation and D) atrial myocyte diameter. Male obese spontaneously hypertensive rats (SHR-ob). Placebo (PLAC). NHE3-inhibitor SAR (SAR). SHR-ob PLAC (n = 8) and SHR-ob SAR (n = 7). All values represented as mean ± SEM. For statistical analysis an unpaired student's *t*-test was performed.

Table 1
Differential Gene Expression of left atrial tissue in SHR-ob PLAC (n = 8) and SHR-ob SAR (n = 7). Transforming growth factor beta 1 (TGFβ1), collagen 1a1 (Col1a1), connective tissue growth factor (CTGF).

Gene expression/ GAPDH	SHR-ob PLAC Mean [%of mean SHR-ob PLAC]	SHR-ob SAR Mean [%of mean SHR-ob PLAC]
TGFβ1	100	79 ± 5*
Col1a1	100	52 ± 12*
CTGF	100	69 ± 9*

* p < 0.01 vs. SHR-ob PLAC.

structural changes, NHE3 inhibitor-treated SHR-ob rats showed improved LA-emptying function parameters, less local atrial conduction disturbances and reduced AF susceptibility.

Total interstitial fibrosis formation was increased in SHR-ob, associated with enhanced myocyte-myocyte distances within bundles of the LA myocardium. An increase in endomysial fibrosis is consistent with changes observed in AF-patients and animal models for AF [16–18]. This extracellular matrix remodeling was associated with local conduction disturbances and impairment of LA-emptying function in SHR-ob rats, which may be a functional consequence of the documented structural atrial changes together with moderate diastolic ventricular dysfunction in SHR-ob [12,15]. Intestinal NHE3 inhibition reduced LA structural alterations, which was associated with the preservation of better LA emptying function and attenuation of increased AF-inducibility and maintenance. However, left atrial function and atrial electrophysiological characteristics previously observed in normotensive rats or spontaneously hypertensive rats could not be achieved in SAR treated SHR-ob [12].

Our study of selective pharmacological NHE3 inhibition in the gut provides important insight into the relevant role of intestinal sodium absorption for the progression of an arrhythmogenic substrate in the atrium. There are several mechanisms how intestinal NHE3 inhibition may prevent AF. Previously, we showed that pharmacological inhibition of intestinal NHE3 using an orally non-absorbable, specific NHE3-inhibitor increased fecal sodium excretion and water content, while circulating sodium concentrations were not altered [9]. This was associated with a sustained reduction in systolic blood pressure, reduced cardiac pre- and afterload and attenuation of cardiac hypertensive end-organ damage in hypertensive rats [9,11]. In addition to these hemodynamic changes, inhibition of NHE3-dependent intestinal sodium absorption results in increased feces sodium concentration and subsequent changes in feces milieu, particularly in the distal ilium and colon, which may critically impact the composition of gut microbiota [19]. High salt intake has been shown to affect the gut microbiome in mice, particularly by depleting Lactobacillus murinus [20]. Treatment of mice with these bacteria prevented salt-sensitive hypertension by modulating autoimmunity [20]. Although we did not study the microbiome after gut-restricted NHE3 inhibition, modulation of the intraluminal intestinal milieu

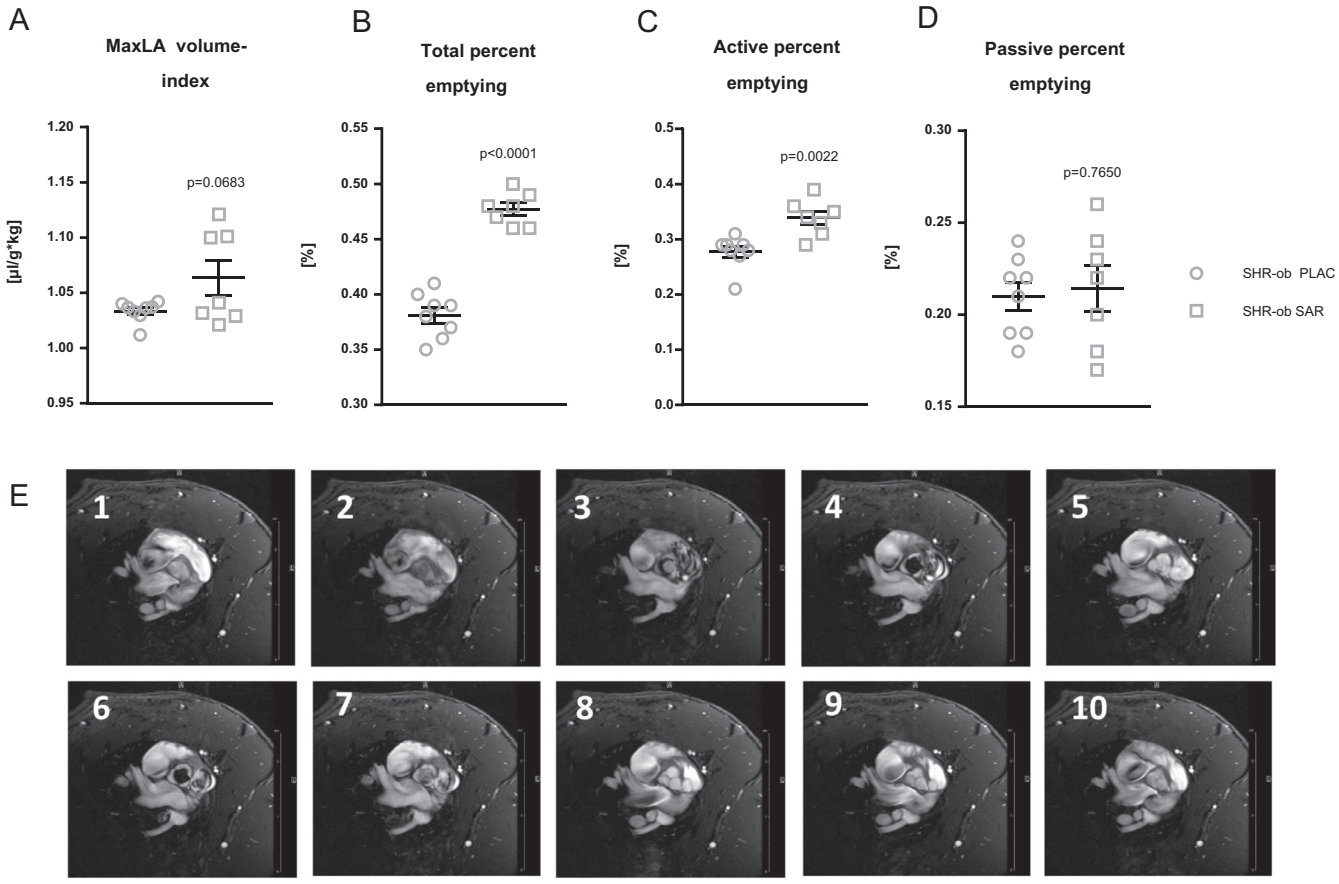

Fig. 2. Quantification of global left atrial (LA) emptying function. Left atrial (LA) emptying function was assessed by magnetic resonance imaging (MRI) in SHR-ob PLAC (n = 8) and SHR-ob SAR (n = 7) rats. Global LA function was assessed by determination of A) maximal LA volume index, B) total percent emptying, C) active percent emptying and D) passive percent emptying. Male obese spontaneously hypertensive rats (SHR-ob). E) Representative MRI images of 10 equal phases throughout the cardiac cycle at the level of the aortic valve are presented. Placebo (PLAC). NHE3-inhibitor SAR (SAR). All values represented as mean ± SEM. For statistical analysis an unpaired student's *t*-test was performed.

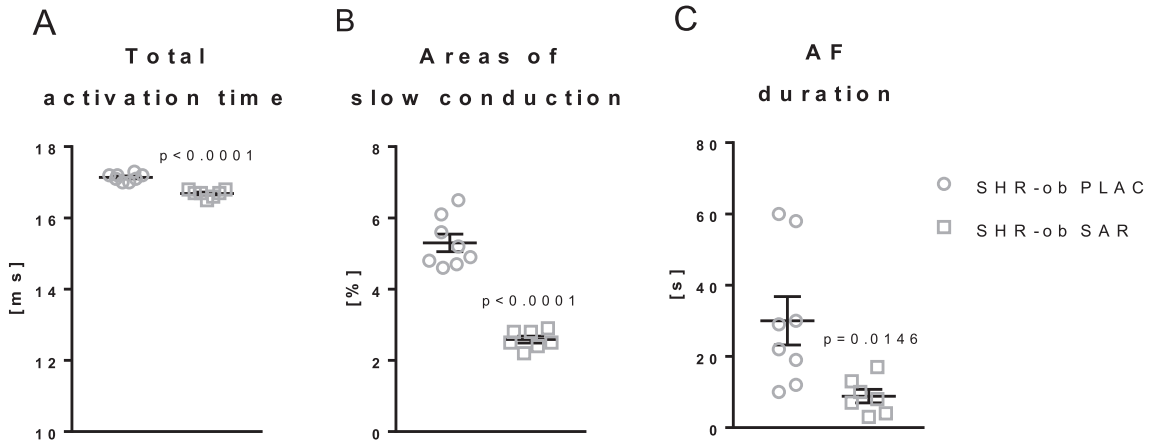

Fig. 3. Left atrial electrophysiological analysis and duration of burst-induced atrial fibrillation. Quantification of A) total atrial activation time and B) areas of slow conduction. C) Duration of inducible episodes of atrial fibrillation (AF). Male obese spontaneously hypertensive rats (SHR-ob). Placebo (PLAC). NHE3-inhibitor SAR (SAR). SHR-ob PLAC (n = 8) and SHR-ob SAR (n = 7). All values represented as mean ± SEM. For statistical analysis an unpaired student's *t*-test was performed.

documented in this study might be a promising approach to influence the composition of gut microorganisms [19,20]. Intestinal NHE3 inhibition may also display some beneficial effects by changes in the neurohumoral system. However, gut-restricted NHE3 inhibition did not impact renin angiotensin aldosterone system activation in spontaneously hypertensive rats [9,10].

Pharmacological intestinal NHE3 inhibition involves several interesting pharmacological strategies and approaches to reduce intestinal sodium absorption [21]. Generally, drugs are designed to be rapidly absorbed to achieve therapeutic plasma levels, and then be eliminated by multiple pathways. In contrast, oral administration of non-absorbable drugs minimize systemic exposure and

exert their therapeutic effects locally in the gastrointestinal tract. Non-absorbable and therefore non-systemic drugs display less off-target systemic effects and thereby less drug-drug interaction, toxicity, or side-effects. In this light, oral administration of highly selective non-absorbable NHE3-inhibitors reduces the intestinal water and sodium absorption in the gut. These inhibitors specifically target the membrane-bound protein-fraction of the NHE3, which is expressed on the cell surface of the gut epithelia.

4.1. Limitation

Herein, we provide the first characterization of the effects of intestinal inhibition of NHE3 in an obese hypertensive rat model on atrial remodeling. We did not observe spontaneous AF episodes and therefore focused on the electrophysiological and histological characterization of left atrial remodeling processes only. Due to tissue size of the small rat atria, we had to focus on histological analysis within this study. We used direct contact mapping to determine local conduction disturbances in the atria, however optical mapping was not performed. An electrophysiological study in the ventricles was not performed, as we focused on the development of an atrial arrhythmic substrate for AF. The identification of the involved mechanisms, particularly the analysis of the gut microbiome and its potential antiarrhythmic effect, warrants further study. Additionally, SHR-ob express hypertension and obesity for their genetic changes and some results from animal experiments cannot be directly extrapolated to humans but can be used to generate hypotheses for future research. The effect of SAR treatment on atrial electrophysiology in normotensive rats with a healthy phenotype is lacking in this study. However, that SAR results in a dose-dependent increase in feces sodium concentration and intestinal water excretion in normotensive rats has been investigated elsewhere [9]. Future pre-clinical and clinical intervention studies should also focus on a potential atrial antiarrhythmic effect of low sodium diet.

4.2. Conclusion

This study is the first to show, that pharmacological inhibition of intestinal sodium absorption displays beneficial effects which are normally expected from dietary interventions, which are often difficult to achieve. Whether pharmacological lifestyle modification by intestinal NHE3-inhibition as investigated in this study in rats or other pharmacological dietary interventions helps to maintain sinus rhythm warrants further studies and future approaches in humans.

Funding

The NHE3-inhibitor SAR was provided by Sanofi Aventis. This work was supported by the German Research Foundation [DFG SFB/TRR219-M02/-S02].

Author contribution

DL, BL and MH conceived and designed research. BL and MH conducted experiments. RM, AS, MH analyzed data. BL, MH, DL, and AS wrote the manuscript. DL, TJ, US, and PS helped in designing, consulting research and project progression and reviewing the manuscript.

Declaration of Competing Interest

The authors declare that they have no known competing financial interests or personal relationships that could have appeared to influence the work reported in this paper.

References

[1] A. Mente, M. O'Donnell, S. Rangarajan, M. McQueen, G. Dagenais, A. Wielgosz, S. Lear, S.T.L. Ah, L. Wei, R. Diaz, A. Avezum, P. Lopez-Jaramillo, F. Lanas, P. Mony, A. Szuba, R. Iqbal, R. Yusuf, N. Mohammadifard, R. Khatib, K. Yusoff, N. Ismail, S. Gulec, A. Rosengren, A. Yusufali, L. Kruger, L.P. Tsolekile, J. Chifamba, A. Dans, K.F. Alhabib, K. Yeates, K. Teo, S. Yusuf, Urinary sodium excretion, blood pressure, cardiovascular disease, and mortality: a community-level prospective epidemiological cohort study, Lancet 392 (10146) (2018) 496–506.

[2] M. O'Donnell, A. Mente, S. Rangarajan, M.J. McQueen, X. Wang, L. Liu, H. Yan, S. F. Lee, P. Mony, A. Devanath, A. Rosengren, P. Lopez-Jaramillo, R. Diaz, A. Avezum, F. Lanas, K. Yusoff, R. Iqbal, R. Ilow, N. Mohammadifard, S. Gulec, A.H. Yusufali, L. Kruger, R. Yusuf, J. Chifamba, C. Kabali, G. Dagenais, S.A. Lear, K. Teo, S. Yusuf, P. Investigators, Urinary sodium and potassium excretion, mortality, and cardiovascular events, New England J. Med. 371 (7) (2014) 612–623.

[3] C. Nishida, R. Uauy, S. Kumanyika, P. Shetty, The joint WHO/FAO expert consultation on diet, nutrition and the prevention of chronic diseases: process, product and policy implications, Public Health Nutr. 7 (1A) (2004) 245–250.

[4] P. Ponikowski, A.A. Voors, S.D. Anker, H. Bueno, J.G.F. Cleland, A.J.S. Coats, V. Falk, J.R. Gonzalez-Juanatey, V.P. Harjola, E.A. Jankowska, M. Jessup, C. Linde, P. Nihoyannopoulos, J.T. Parissis, B. Pieske, J.P. Riley, G.M.C. Rosano, L.M. Ruilope, F. Ruschitzka, F.H. Rutten, P. van der Meer, E.S.C.S.D. Group, 2016 ESC Guidelines for the diagnosis and treatment of acute and chronic heart failure: The Task Force for the diagnosis and treatment of acute and chronic heart failure of the European Society of Cardiology (ESC)Developed with the special contribution of the Heart Failure Association (HFA) of the ESC, Eur. Heart J. 37 (27) (2016) 2129–2200.

[5] B. Williams, G. Mancia, W. Spiering, E. Agabiti Rosei, M. Azizi, M. Burnier, D.L. Clement, A. Coca, G. de Simone, A. Dominiczak, T. Kahan, F. Mahfoud, J. Redon, L. Ruilope, A. Zanchetti, M. Kerins, S.E. Kjeldsen, R. Kreutz, S. Laurent, G.Y.H. Lip, R. McManus, K. Narkiewicz, F. Ruschitzka, R.E. Schmieder, E. Shlyakhto, C. Tsioufis, V. Aboyans, I. Desormais, E.S.C.S.D. Group, 2018 ESC/ESH Guidelines for the management of arterial hypertension, Eur. Heart. J. (2018) 71–159, https://doi.org/10.5603/KP.2019.0018.

[6] Paulus Kirchhof, Stefano Benussi, Dipak Kotecha, Anders Ahlsson, Dan Atar, Barbara Casadei, Manuel Castella, Hans-Christoph Diener, Hein Heidbuchel, Jeroen Hendriks, Gerhard Hindricks, Antonis S. Manolis, Jonas Oldgren, Bogdan Alexandru Popescu, Ulrich Schotten, Bart Van Putte, Panagiotis Vardas, Stefan Agewall, John Camm, Gonzalo Baron Esquivias, Werner Budts, Scipione Carerj, Filip Casselman, Antonio Coca, Raffaele De Caterina, Spiridon Deftereos, Dobromir Dobrev, José M. Ferro, Gerasimos Filippatos, Donna Fitzsimons, Bulent Gorenek, Maxine Guenoun, Stefan H. Hohnloser, Philippe Kolh, Gregory Y.H. Lip, Athanasios Manolis, John McMurray, Piotr Ponikowski, Raphael Rosenhek, Frank Ruschitzka, Irina Savelieva, Sanjay Sharma, Piotr Suwalski, Juan Luis Tamargo, Clare J. Taylor, Isabelle C. Van Gelder, Adriaan A. Voors, Stephan Windecker, Jose Luis Zamorano, Katja Zeppenfeld, 2016 ESC Guidelines for the management of atrial fibrillation developed in collaboration with EACTS, Europace 18 (11) (2016) 1609–1678, https://doi.org/10.1093/europace/euw295.

[7] R.D. Mattes, D. Donnelly, Relative contributions of dietary sodium sources, J. Am. Coll. Nutr. 10 (4) (1991) 383–393.

[8] E.M. Bradford, M.A. Sartor, L.R. Gawenis, L.L. Clarke, G.E. Shull, Reduced NHE3-mediated Na+ absorption increases survival and decreases the incidence of intestinal obstructions in cystic fibrosis mice, Am. J. Physiol. Gastrointest. Liver Physiol. 296 (4) (2009) G886–G898.

[9] D. Linz, K. Wirth, W. Linz, H.O. Heuer, W. Frick, A. Hofmeister, U. Heinelt, P. Arndt, U. Schwahn, M. Bohm, H. Ruetten, Antihypertensive and laxative effects by pharmacological inhibition of sodium-proton-exchanger subtype 3-mediated sodium absorption in the gut, Hypertension 60 (6) (2012) 1560–1567.

[10] A.G. Spencer, E.D. Labonte, D.P. Rosenbaum, C.F. Plato, C.W. Carreras, M.R. Leadbetter, K. Kozuka, J. Kohler, S. Koo-McCoy, L. He, N. Bell, J. Tabora, K.M. Joly, M. Navre, J.W. Jacobs, D. Charmot, Intestinal inhibition of the Na+/H+ exchanger 3 prevents cardiorenal damage in rats and inhibits Na+ uptake in humans, Sci. Transl. Med. 6 (227) (2014) 227ra36.

[11] B. Linz, M. Hohl, J.C. Reil, M. Bohm, D. Linz, Inhibition of NHE3-mediated sodium absorption in the gut reduced cardiac end-organ damage without deteriorating renal function in obese spontaneously hypertensive rats, J. Cardiovasc. Pharmacol. 67 (3) (2016) 225–231.

[12] M. Hohl, D.H. Lau, A. Muller, A.D. Elliott, B. Linz, R. Mahajan, J.M.L. Hendriks, M. Bohm, U. Schotten, P. Sanders, D. Linz, Concomitant obesity and metabolic syndrome add to the atrial arrhythmogenic phenotype in male hypertensive rats, J. Am. Heart Assoc. 6 (9) (2017).

[13] D. Linz, M. Hohl, F. Mahfoud, J.C. Reil, W. Linz, T. Hubschle, H.P. Juretschke, C. Neumann-Haflin, H. Rutten, M. Bohm, Cardiac remodeling and myocardial dysfunction in obese spontaneously hypertensive rats, J. Transl. Med. 10 (2012) 187.

[14] D. Linz, M. Hohl, J. Schutze, F. Mahfoud, T. Speer, B. Linz, T. Hubschle, H.P. Juretschke, R. Dechend, J. Geisel, H. Rutten, M. Bohm, Progression of kidney injury and cardiac remodeling in obese spontaneously hypertensive rats: the role of renal sympathetic innervation, Am. J. Hypertens. 28 (2) (2015) 256–265.

[15] S.R. Selejan, D. Linz, A.M. Tatu, M. Hohl, T. Speer, S. Ewen, F. Mahfoud, I. Kindermann, O. Zamyatkin, A. Kazakov, U. Laufs, M. Bohm, Sympathoadrenergic suppression improves heart function by upregulating the ratio of sRAGE/RAGE in hypertension with metabolic syndrome, J. Mol. Cell. Cardiol. 122 (2018) 34–46.

[16] D. Linz, M. Hohl, S. Dhein, S. Ruf, J.C. Reil, M. Kabiri, P. Wohlfart, S. Verheule, M. Bohm, T. Sadowski, U. Schotten, Cathepsin A mediates susceptibility to atrial tachyarrhythmia and impairment of atrial emptying function in Zucker diabetic fatty rats, Cardiovasc. Res. 110 (3) (2016) 371–380.

[17] M. Hohl, K. Erb, L. Lang, S. Ruf, T. Hubschle, S. Dhein, W. Linz, A.D. Elliott, P. Sanders, O. Zamyatkin, M. Bohm, U. Schotten, T. Sadowski, D. Linz, Cathepsin a mediates ventricular remote remodeling and atrial cardiomyopathy in rats with ventricular ischemia/reperfusion, JACC Basic Transl. Sci. 4 (3) (2019) 332–344.

[18] S. Verheule, E. Tuyls, A. Gharaviri, S. Hulsmans, A. van Hunnik, M. Kuiper, J. Serroyen, S. Zeemering, N.H. Kuijpers, U. Schotten, Loss of continuity in the thin epicardial layer because of endomysial fibrosis increases the complexity of atrial fibrillatory conduction, Circ. Arrhythm. Electrophysiol. 6 (1) (2013) 202–211.

[19] R.S. Mishima, M. Hohl, B. Linz, P. Sanders, D. Linz, Too fatty, too salty, too western, Hypertension 72 (5) (2018) 1078–1080.

[20] N. Wilck, M.G. Matus, S.M. Kearney, S.W. Olesen, K. Forslund, H. Bartolomaeus, S. Haase, A. Mahler, A. Balogh, L. Marko, O. Vvedenskaya, F.H. Kleiner, D. Tsvetkov, L. Klug, P.I. Costea, S. Sunagawa, L. Maier, N. Rakova, V. Schatz, P. Neubert, C. Fratzer, A. Krannich, M. Gollasch, D.A. Grohme, B.F. Corte-Real, R.G. Gerlach, M. Basic, A. Typas, C. Wu, J.M. Titze, J. Jantsch, M. Boschmann, R. Dechend, M. Kleinewietfeld, S. Kempa, P. Bork, R.A. Linker, E.J. Alm, D.N. Muller, Salt-responsive gut commensal modulates TH17 axis and disease, Nature 551 (7682) (2017) 585–589.

[21] A.G. Spencer, P.J. Greasley, Pharmacologic inhibition of intestinal sodium uptake: a gut centric approach to sodium management, Curr. Opin. Nephrol. Hypertens. 24 (5) (2015) 410–416.